



**HAL**  
open science

## **Visualizing Retinotopic Half-Wave Rectified Input to the Motion Detection Circuitry of Drosophila.**

Dierk Frithjof Reiff, Johannes Plett, Marco Mank, Oliver Griesbeck, Alexander A Borst

► **To cite this version:**

Dierk Frithjof Reiff, Johannes Plett, Marco Mank, Oliver Griesbeck, Alexander A Borst. Visualizing Retinotopic Half-Wave Rectified Input to the Motion Detection Circuitry of Drosophila.. Nature Neuroscience, 2010, <10.1038/nn.2595>. <hal-00554657>

**HAL Id: hal-00554657**

**<https://hal.science/hal-00554657v1>**

Submitted on 11 Jan 2011

**HAL** is a multi-disciplinary open access archive for the deposit and dissemination of scientific research documents, whether they are published or not. The documents may come from teaching and research institutions in France or abroad, or from public or private research centers.

L'archive ouverte pluridisciplinaire **HAL**, est destinée au dépôt et à la diffusion de documents scientifiques de niveau recherche, publiés ou non, émanant des établissements d'enseignement et de recherche français ou étrangers, des laboratoires publics ou privés.



HAL Authorization

## Visualizing Retinotopic Half-Wave Rectified Input to the Motion Detection Circuitry of *Drosophila*.

Dierk F. Reiff\*, Johannes Plett, Marco Mank, Oliver Griesbeck and Alexander Borst

Max-Planck-Institute of Neurobiology, Martinsried, Germany

\* corresponding author's address:

Department of Systems and Computational Neurobiology

Max-Planck-Institute of Neurobiology

D-82152, Martinsried, Germany

Tel: +49 89 8578 3254

Fax: +49 89 8578 3252

email: [reiff@neuro.mpg.de](mailto:reiff@neuro.mpg.de)

### ABSTRACT

In the visual system of *Drosophila*, photoreceptors R1-6 relay achromatic brightness information to five parallel pathways. Two of them, the lamina monopolar cells L1 and L2, represent the major input lines to the motion detection circuitry. Here we devised a new method for the optical recording of visually evoked changes in intracellular  $\text{Ca}^{2+}$  in neurons, using targeted expression of a genetically encoded  $\text{Ca}^{2+}$  indicator.  $\text{Ca}^{2+}$  in single terminals of L2 neurons in the medulla carries no information about the direction of motion. However, the observed strong increase in intracellular  $\text{Ca}^{2+}$  induced by light-OFF and only small changes induced by light-ON suggest half-wave rectification of the input signal. Thus, L2 predominantly transmits brightness decrements to downstream circuits that then compute the direction of image motion.

## INTRODUCTION

The fly visual system continuously provides information about the motion of objects, conspecifics, predators and the 3D-structure of the environment. This information underlies the execution of remarkable visually driven behaviours<sup>1-4</sup>. Yet, how small scale neural networks accomplish such computational efficacy remains an open question, and in no animal has the complete motion detection circuitry been revealed so far<sup>5,6</sup>. Here, we pursue this question in *Drosophila* by analyzing how brightness changes become encoded in changes in the concentration of presynaptic calcium ( $\text{Ca}^{2+}$ ) in the axon terminals of L2 neurons, a major input channel to the motion detection circuitry<sup>7-10</sup>.

The processing of brightness changes underlies the detection of visual motion. Based on a detailed input-output analysis of the optomotor response in tethered beetles, the well-known Hassenstein-Reichardt-Model (HRM) of visual motion detection was derived<sup>11,12</sup>. The HRM (**Supplementary Fig. 1a**) essentially performs a spatio-temporal cross-correlation of two luminance input signals by multiplying the signals derived from two neighbouring image points after one of them has been temporally delayed. This operation is executed in each of two mirror symmetrical half-detectors that operate with opposite sign. Summing the output of both half-detectors results in a directionally selective response of the full detector. Notably, the HRM precisely describes in algorithmic terms the observed optomotor behaviour of walking beetles and walking and flying flies<sup>12,13</sup>. Furthermore, the fundamental computations of the HRM can explain motion detection in different vertebrate species including man<sup>14-17</sup>. In flies, directionally selective responses that closely match the predictions of the model were observed in the large tangential neurons of both (reviewed in<sup>18</sup>) large fly species (reviewed in<sup>5</sup>) and *Drosophila*<sup>19,20</sup>. These cellular responses carry distinct signatures that derive from the correlative processing within the HRM<sup>12</sup> (reviewed in<sup>5,6,18</sup>).

However, because of the purely algorithmic nature of the HRM, no immediate conclusions about the underlying neuronal hardware can be drawn: Different implementations of the model can result in similar output. Aiming for insights into the cellular implementation of the model<sup>21-23</sup> extracellular responses of the directionally selective H1 neuron were recorded while presenting apparent motion stimuli<sup>24</sup>: Sequential stimulation of individual photoreceptor pairs (R1 and R6)<sup>23</sup> of the same ommatidium led to the proposal that each input signal is split into an ON- and an OFF-channel which then feed into separate multipliers for the processing of brightness increments and decrements, respectively<sup>22,23</sup> (**Supplementary Fig. 1b**). However, interactions among brightness increments and decrements are inherent to the original HRM<sup>12</sup> (**Supplementary Fig. 1a**) and were repeatedly observed in behavioural optomotor responses<sup>12</sup> as well as in the cellular responses of the H1 neuron<sup>21</sup>: Apparent motion stimuli with opposite polarity induce responses that report a reversal of the true direction of the stimulus<sup>21</sup>, a phenomenon known in psychophysics as ‘reverse-phi’<sup>25</sup>. If a neuron is assumed to perform a multiplication in a sign-correct manner this neuron’s output signal should increase in a supra-linear way when both inputs increase as well as when both inputs decrease. To our knowledge, no biologically plausible mechanism is known that could accomplish such

a computation. In order to get closer to a possible cellular implementation, Hassenstein and Reichardt<sup>12</sup> proposed a circuit (**Supplementary Fig. 1c**) that was inspired by the “Four-Quadrant-Multiplier” used in analog signal processing: Bipolar (positive as well as negative signal components) input signals are half-wave rectified resulting in positive signals only. These signals are subsequently processed in four separate multipliers accounting for all possible interactions (ON-ON, ON-OFF, OFF-ON, OFF-OFF). The output of the individual multipliers is then summed by a postsynaptic integrator in a sign-correct manner. From the perspective of this integrator, the models in **Supplementary Fig. 1a** and **1c** are mathematically identical. Thus, in contrast to a previous account<sup>21</sup>, separate input channels for the processing of brightness increments and decrements cannot be excluded based on responses to mixed input signals.

In flies, the lamina monopolar neurons L1 and L2 are the largest and best investigated second order visual interneurons postsynaptic to the photoreceptors R1-6<sup>26-29</sup>. L1-L3 and amc all express a chloride channel encoded by the gene *ort*<sup>30</sup> which is gated by the photoreceptor transmitter histamine<sup>31,32</sup>. The processes of amacrine cells stay in the lamina where they synapse onto L5, and L4 receives input from L2 (and feeds back onto two more lateral L2 neurons)<sup>29</sup>. L4 and L5, as well as L1-3 project to distinct layers in the medulla<sup>26</sup>. Thus, five possible parallel processing streams (three direct channels: L1-L3; two indirect channels L4 and L5) transmit information about brightness changes from the lamina<sup>29</sup> to the medulla<sup>26</sup>. Behavioural and genetic experiments suggest that L3 is involved in processing of UV-light and in phototaxis<sup>9</sup>. In contrast, L1 and L2 provide the major input to the motion detection circuitry in the medulla<sup>7-10</sup>. Recordings of their dendritic membrane potential revealed non-directional, strongly adapting responses in large fly species<sup>33</sup>: Dendritic voltage changes in L1 and L2 to a transient light pulse correspond to an inverted, high-pass filtered biphasic version of the voltage change recorded in photoreceptors<sup>33-36</sup> that depolarize in response to light. The reported inhibitory current through histamine gated chloride channels<sup>32</sup> explains the hyperpolarizing ON-response<sup>37</sup>, however, it does not explain the excitatory OFF-component at the end of a light pulse that has been observed in large flies<sup>33-37</sup>. In *Drosophila* depolarizing voltage responses to light-OFF have not been observed<sup>38</sup>.

Even though there have been electrophysiological studies on lamina monopolar cells and few other columnar neurons in *Calliphora*<sup>39,40</sup>, the signals that are transmitted by lamina monopolar cells to neurons of the motion detection circuitry in the medulla<sup>41</sup> could not be recorded so far for methodological reasons. Here, we address this problem in fly motion vision by investigating how L2 axon terminals in the medulla<sup>26</sup> encode brightness changes in presynaptic intracellular calcium. Visually evoked  $\text{Ca}^{2+}$  is measured by a new method that employs optical recording of the genetically encoded calcium indicator TN-XXL<sup>42</sup> targeted to L2 neurons and an interlaced visual stimulation technique.

## RESULTS

### Functional Two-Photon imaging in the *Drosophila* visual system

We targeted the expression of the dual chromophore calcium indicator TN-XXL<sup>42</sup> to the about 750 non-spiking L2 lamina monopolar cells of the visual system of *Drosophila* using the enhancer trap line '21D-Gal4'<sup>7</sup> (**Fig. 1**). L2 neurons were chosen based on the availability of this specific Gal4-driver line and the supposed pivotal role of L2 in visual motion detection<sup>6-10</sup>. Visually-evoked spatio-temporal changes in  $\text{Ca}^{2+}$  in the highly ordered<sup>27,28</sup>, retinotopically organized lattice of L2 axon terminals<sup>7</sup> (**Fig. 1b-d**) were monitored using 'Two-Photon Laser Scanning Microscopy' (2PLSM)<sup>43</sup> (**Fig. 1a**). Two-photon excitation of photoreceptors was prevented as two-photon excitation is confined<sup>43,44</sup> to a small volume in the focal plane of the objective that was kept distant from the photoreceptor layer. Furthermore, one-photon excitation of *Drosophila's* photoreceptors by laser light ( $\lambda = 825$  nm) was prevented by reducing the laser power to a maximum of 10 mW. As a typical value, 5 mW was measured at the specimen.

Another technical problem of calcium imaging during visual stimulation of the fly's eye lies in protecting the photomultiplier tubes from light originating from the visual stimulus (**Fig. 1e**). We achieved this by fast switching of a custom built LED panel display synchronized to the movement of the horizontal scanning mirror of the 2PLSM (**Fig. 1a,e**). This design allowed us to separate the recording of TN-XXL fluorescence and the presentation of visual stimuli in time. We used 2 ms scan time per line, of which 400  $\mu\text{s}$  were spent on the fly-back period of the horizontal scanning mirror. 330  $\mu\text{s}$  of this fly-back time were used to gate the LEDs. This resulted in a visual stimulus flickering at 500 Hz which is far beyond the temporal resolution of *Drosophila* photoreceptors<sup>45</sup> and thus should be perceived as continuous light (60 cd / m<sup>2</sup> during light ON).

### ON-OFF processing in the L2 pathway

We investigated how whole-field increments and decrements in brightness are encoded in L2 axon terminal  $\text{Ca}^{2+}$  in the medulla. Therefore, we recorded TN-XXL fluorescence changes in small arrays of up to six individually identifiable L2 axon terminals (**Fig. 2a,b**) per image sequence. We observed small non-uniform changes in  $\text{Ca}^{2+}$  induced by light-ON: In one set of experiments (**Fig. 2c**) a single, spatially uniform pulse of light (8 sec duration, dark adapted eye, recordings interspersed by 60 sec darkness) elicited a small, slow increase in  $\text{Ca}^{2+}$  at the onset of the light pulse. However, in other experiments, we observed a small negative change in  $\text{Ca}^{2+}$  induced by light-ON (**Fig. 2d**). In contrast, brightness decrements induced a uniform, strong and long-lasting increase in  $\text{Ca}^{2+}$ . This calcium signal, induced by light-OFF, can be fit by single exponential functions with a time constant of  $\tau = 0.22 - 0.26$  s for the rise (not shown) and 2.10 s for the decay (**Fig. 2e**). The strong increase in  $\text{Ca}^{2+}$  in response to light-OFF suggests an inversion and half-wave rectification of the input signal in L2 axon terminals.

Changes in  $\text{Ca}^{2+}$  induced by individual light-OFF stimuli might superimpose in a linear way during periodic flicker. Alternatively, light-ON might affect the observed increase in calcium induced by light-OFF. We analyzed this question (**Fig. 2d**) and found that increased  $\text{Ca}^{2+}$  in response to brightness decrements was effectively

reduced to baseline by following brightness increments (compare black trace and colored traces in **Fig. 2d**). This finding is reflected in a much shorter time constant of the decay of this truncated calcium signal ( $\tau = 0.26$  s compared to 2.10 s; **Fig. 2e**) that was the same for all inter-pulse intervals tested (0.26 - 1.16 sec, **Fig. 2d,e**). Furthermore, brightness increments presented before the response to the preceding brightness decrement reached its maximum, reduced the amplitude of the  $\text{Ca}^{2+}$  signal (**Fig. 2d**, green trace). Thus, L2-terminals are sensitive to brightness increments: there is a small non-uniform calcium signal induced by light-ON in the dark-adapted state, as well as a rapid reduction in  $\text{Ca}^{2+}$  if presynaptic  $\text{Ca}^{2+}$  is elevated from a preceding decrement in brightness.

We further tested the encoding of subsequent brightness increments and decrements in  $\text{Ca}^{2+}$  by stimulating the eye of the fly with light flickering at 0.25 Hz (**Fig. 2f**) and 1 Hz (**Fig. 2g**). As expected, the L2 terminal  $\text{Ca}^{2+}$  rose in response to brightness decrements and was rapidly reduced to baseline by subsequent brightness increments. A full modulation of  $\text{Ca}^{2+}$  with maximum increase and full return to baseline was exhibited at 0.25 Hz (**Fig. 2f**) whereas switching between brightness increments and decrements every 500 ms (1 Hz stimulus) led to a smaller modulation of  $\text{Ca}^{2+}$  superimposed on a DC component (**Fig. 2g**). These experiments suggest that light-OFF- $\text{Ca}^{2+}$  and its rapid reduction by light-ON represent the main signal transmitted by L2. However, our experiments cannot reveal the frequency range that is transmitted by L2 axon terminals as binding to and unbinding of calcium from TN-XXL results in significant low-pass filtering of the unperturbed calcium signal<sup>42</sup> (see  $\tau$  in **Fig. 2e**).

### Moving visual stimuli

Drifting visual gratings elicit modulations of the photoreceptor potential independent of the direction of motion. In contrast, tangential cells in the third neuropile of the optic lobe, the lobula plate, exhibit directionally selective responses (reviewed in<sup>5,18</sup>). These directionally selective cells are supposed key players in the control of visually driven optomotor behaviour. In recent behavioural experiments<sup>9</sup> flies lacking the lamina neurons L1 and L2 were shown to be motion blind<sup>7,8</sup>, and flies with L4-cells specifically blocked were reported to be motion blind. Furthermore, anatomical connections within the lamina<sup>7,29</sup> suggested involvement of L2 and L4 in a direction selective pathway with higher sensitivity for the detection of front-to-back motion<sup>7</sup>. However, during the presentation of moving visual stimuli to the eye, the output signals of L1 and L2 cells in the medulla have not been analyzed so far. Thus, we next investigated whether the calcium signals in L2 axon terminals in the medulla carry any sign of motion, orientation or direction selectivity, or whether they transmit signals that purely encode local luminance changes.

We presented visual gratings of 30 deg spatial wavelength moving at 30 deg / sec, resulting in 1 Hz temporal frequency, in four orthogonal directions (**Fig. 3**). Time-locked to the visual stimuli, we recorded fluorescence changes from groups of individually identifiable L2-terminals within the same depth of the medulla (fly head and recording situation shown in **Fig. 3a** and **Fig. 1**). The L2 terminals were oriented

along the dorso-ventral axis (**Fig. 3a–c,f**). Grating motion elicited fluorescence-modulations in the individual L2 terminals at a frequency of 1 Hz, for all directions of motion. When motion was along the dorso-ventral axis, modulations in neighbouring terminals were phase-shifted by  $\pi/3$  (**Fig. 3d**), corresponding nicely to the relationship between the interommatidial angle of about 5 deg in *Drosophila*<sup>13</sup> and the 30 deg spatial wavelength of the stimulus, i.e. 1/6. In contrast, motion along the horizontal axis elicited synchronous oscillations in neighbouring L2-terminals of the same vertical row (**Fig. 3e**) as expected from their vertically aligned receptive fields (**Fig. 3a**).

Front-to-back and back-to-front motion at a temporal frequency of 1 Hz elicited changes in  $\text{Ca}^{2+}$  that could not be distinguished from changes in  $\text{Ca}^{2+}$  induced by spatially homogeneous flicker at the same frequency (**Fig. 3f**). In sum, these results suggest that  $\text{Ca}^{2+}$  in L2 terminals predominantly encodes decrements in local brightness, irrespective of the direction of motion. This information is transmitted to postsynaptic neurons in the medulla while retaining the original resolution of the *Drosophila* compound eye<sup>13</sup>.

### Blocking photoreceptor transmission to parallel processing streams in the lamina

In the lamina, photoreceptor signals from R1-6 are transmitted to four different cell types (**Fig. 4a**). In order to test if interactions between the different lamina cell types contribute to the observed calcium signals in L2, we investigated flies where L2 neurons are the only interneurons that receive direct input from the photoreceptors<sup>7</sup>. In these 'L2-rescue' flies, TN-XXL and the wild-type histamine receptor were specifically expressed in L2 neurons in a histamine receptor null-mutant<sup>7</sup> (*ort<sup>1</sup>/ort<sup>US2515</sup>; 21D-Gal4; UAS-ort*). As a control, *ort<sup>1</sup>/ort<sup>US2515</sup>* animals without L2 rescue did not show any transients in the electroretinogram (such transients at the begin and at the end of a light pulse reflect L1 and L2 activity<sup>46</sup>), were motion blind, and their tangential cells in the lobula plate did not respond to large field motion stimuli (data not shown), suggesting that photoreceptor to lamina transmission is completely blocked<sup>7,46</sup>. In L2-rescue flies, a brightness decrement induced a strong and long-lasting increase in  $\text{Ca}^{2+}$  that was immediately reduced by a subsequent brightness increment (**Fig. 4b**). However, compared to wild-type flies, the time course of the recorded calcium signal in L2 axon terminals was slowed down. The time-constants of the rise and the decay of  $\text{Ca}^{2+}$  were 0.80 and 6.36 sec, respectively (compared to ~0.26 sec and 2.1 sec, **Fig. 2**). The time constant for the decay in the presence of a subsequent brightness increment was reduced to 0.34 sec (**Fig. 4c**). These experiments suggest that photoreceptor-to-L2 signaling and processing within L2 neurons is sufficient to qualitatively generate the observed changes in  $\text{Ca}^{2+}$ . However, we cannot exclude that L2 elicits activity in the surrounding medulla or neighbouring lamina cells. Such feedback network activity could contribute to the observed characteristics of  $\text{Ca}^{2+}$ . Notably, the increased time constants for the rise and decay in the L2-rescue flies suggest that photoreceptor-to-lamina signaling in parallel channels is required for fast and temporally precise

signaling. The signals transmitted by L1 and L2 as well as the role of interactions among both pathways are currently being investigated in our lab.

## DISCUSSION

L2-cells have been implicated as major input elements to the motion detection circuitry in flies<sup>7-10</sup>. Our data on L2 terminal  $\text{Ca}^{2+}$  suggests an inversion and half-wave rectification (**Fig. 2c,d**) of the brightness signal. Taking into account the role of  $\text{Ca}^{2+}$  in presynaptic vesicle release, we propose that L2 mainly transmits the information about brightness decrements to the motion detection circuit in the medulla.

As dendritic recordings of L2 membrane potential in large flies show at least small depolarizing responses induced by light-OFF<sup>33-37</sup>, the underlying processing likely involves an amplification of the positive dendritic membrane potential and opening of voltage activated calcium channels in L2 terminals induced by light-OFF. Light-ON hyperpolarizes the L2 membrane potential<sup>33-37</sup> which might rapidly inactivate the calcium channels. Efficient calcium extrusion then likely mediates the observed rapid return of the calcium signal to baseline induced by light-ON<sup>33</sup>.

Non-linear processing steps represent a key feature of second order visual interneurons in flies<sup>33-36</sup> as well as in the vertebrate retina: vertebrate ON- and OFF-bipolar cells preferentially relay either increments or decrements in brightness<sup>47</sup>. However, half-wave rectification in bipolar cells is not complete and partly results from inhibitory interactions among ON- and OFF-channels<sup>48-49</sup>. The increase of the time constant observed in L2-rescue flies (**Fig. 4b,c**) and current experiments in our lab suggests that interactions between different lamina cell types are involved in the generation of imperfectly half-wave rectified light-OFF calcium responses in L2 axon terminals. Such interactions are also suggested by the rich anatomical connections at the level of the dendrites within in the lamina<sup>29</sup> as well as at the level of the axon terminals in the medulla<sup>26,27</sup>. Furthermore, given that L2 terminals transmit their main signal at light-OFF, other channels must exist for the signaling of brightness increments<sup>22,23</sup>. Such ON and OFF signaling is a common motif in different animals and sensory modalities<sup>50</sup>. Thus, although not necessary for Hassenstein-Reichardt-type computations<sup>21</sup> (**Supplementary Fig. 1**), half-wave rectifying the input signals into parallel ON- and OFF-channels and multiplying each pair separately allows treating the outputs in a sign-correct way<sup>12</sup> (**Supplementary Fig. 1c**). The devised imaging approach should pave the way for future studies that ultimately reveal the cellular implementation of the Hassenstein-Reichardt-Model of visual motion detection.

## Acknowledgements

We are very grateful to Winfried Denk, Michael Mueller and Juergen Tritthardt (all MPI Heidelberg) for supporting and troubleshooting 2PLSM; to Maximilian Joesch for

providing Matlab code and discussion; to Juergen Haag and Bettina Schnell for discussion and comments on the manuscript; to Wolfgang Essbauer and Christian Theile for technical assistance; to Tim Gollisch for comments on the manuscript (all MPI Martinsried), to Gero Misenboeck (Oxford, UK) and Lucas Sjulsion (Rockefeller University, NY) for their input on the use of LEDs, and to the members of the mechanics and electronics workshop of the MPI Martinsried for excellent support.

### **Author Contributions**

DFR conceptualized the triggered stimulus presentation, JP designed and engineered the LED arena, MM and OG engineered TN-XXL, AB and DFR designed experiments and wrote the manuscript, DFR performed all fly work, all imaging experiments, data analysis and prepared the figures.

**Figure 1.** Experimental approach used for the recording of visually-evoked changes in  $\text{Ca}^{2+}$  in visual interneurons of *Drosophila*. The genetically encoded calcium indicator TN-XXL<sup>42</sup> is targeted to L2 neurons. Fluorescence changes are recorded by Two-Photon Laser Scanning Microscopy (2PLSM) combined with visual stimulation during the flyback time of the x-scanning mirror. (a) A *Drosophila* fly is placed under a water immersion objective<sup>19</sup> attached to a custom built 2PLSM. The fly is looking at a computer controlled LED arena. (b) A piece of cuticle of about 0.3 mm<sup>2</sup> has been removed from the backside of the fly head (outline indicated by the dashed line). The superposition of a wide field image of the exposed brain with TN-XXL fluorescence reveals expression of TN-XXL in the lateral posterior optic lobe (CCD camera images). (c) Close-up at the position of the outer medulla (CCD images as in b), the arrow points at an individual L2 axon terminal. (d) *In vivo* 2-Photon imaging reveals the retinotopic arrangement of L2 axon terminals in layer 2 of the medulla<sup>26</sup>. In the fly optic lobe, the calcium indicator is almost exclusively<sup>7</sup> expressed in L2 neurons (*21D-Gal4*<sup>7</sup> / *UAS-TN-XXL*<sup>42</sup>). Each visual sampling unit is innervated by one L2 axon terminal (arrow). L2 cell bodies (asterisk) lie in the lamina cortex. The dendrites (arrow head) of L2 cells span the entire lamina. Individual images were chosen from an image stack ( $\Delta z$  / image = 1  $\mu\text{m}$ ) and are separated along the z-axis by about 20  $\mu\text{m}$  (scale bar: 30  $\mu\text{m}$ ). (e) Temporal separation of optical recording and visual stimulus presentation circumvents contamination of the recorded fluorescence signal by light from the visual stimulus. A computer controlled LED-arena is precisely synchronized to the movement of the horizontal scanning mirror of the 2PLSM. During the scan (1.6 ms / line) all LEDs are switched off. The LEDs are switched on for 330  $\mu\text{s}$  during the fly-back period of the horizontal scanning mirror (400  $\mu\text{s}$ ). CFP and YFP: Cyan- and Yellow Fluorescent Protein, respectively.

**Figure 2.** Visually-evoked changes in  $\text{Ca}^{2+}$  in L2 axon terminals in the medulla of *Drosophila*. (a) TN-XXL expressing L2 axon terminals form a retinotopic map (asterisk) in layer 2 of the medulla (arrow: ommatidial lenses and cuticle; arrow head: air sacs). (b) Typical recording situation: Four individually identifiable neighbouring L2 terminals and their axon are shown. Recorded data are shown in c–g. (c) Light-OFF of a spatially homogeneous pulse of light (8 sec) induces a uniform, strong increase in presynaptic  $\text{Ca}^{2+}$  with slow decay (arrow). Light-ON (asterisk) induced either a small increase (c) or decrease (d) in  $\text{Ca}^{2+}$  (5 animals,  $n = 88$  recorded image sequences in c). (d)  $\text{Ca}^{2+}$  induced by the end of the first light pulse (1) is quickly reduced (black arrow) to baseline by the onset of a subsequent light pulse (2). Colored traces show the mean calcium response in the presence of a second pulse of light (inter stimulus interval  $\Delta t$ : blue 1.16 s; orange 0.86 s; red 0.56 s; green 0.26 s; black only first pulse; 4 animals,  $n = 33, 29, 41, 34$  and  $33$  image sequences). The variability in the response is comparable to the results shown in panel c, f and g. (e) 8-fold decrease of the time constant for the decay of  $\text{Ca}^{2+}$  in the presence of subsequent light-ON:  $\tau = 2.1$  s for a single pulse of light ( $R = 0.98$ , upper trace) and  $\tau = 0.26$  s for the “truncated”  $\text{Ca}^{2+}$  response ( $R = 0.92$ , lower trace,  $\Delta t = 0.56$  s). The time course of the  $\text{Ca}^{2+}$  signal was fitted by a single exponential function (red traces). (f) Stimulus: 0.25 Hz flicker. The modulation of  $\text{Ca}^{2+}$  is in phase with the flicker frequency of the stimulus ( $n = 4$  animals / 50 image sequences). (g) Decreasing modulation depth of  $\text{Ca}^{2+}$  at a stimulus (flicker) frequency of 1 Hz and appearance of a tonic signal component ( $n = 3$  animals / 53 image sequences). Scale bar 20  $\mu\text{m}$  in (a) and 10  $\mu\text{m}$  in (b). Mean (black), standard error (grey) in c, f and g.

**Figure 3.** Neural signature of drifting visual gratings: Changes in  $\text{Ca}^{2+}$  in retinotopically organized L2 terminals reflect the spatio-temporal layout of the visual stimulus. (a) Schematic drawing of the fly head and optic lobe during recording; caudal is facing upward (see **Fig. 1**). Photoreceptors located in a vertical column of frontal ommatidia (shown in red) send their axon to L2-cells that connect the lamina to the caudal medulla (neuropile shown in brown). (b) Precise alignment of the fly head allows 2-Photon imaging of the corresponding row of L2-axon terminals in layer 2 of the medulla. (c) Five individually identifiable, neighbouring terminals were recorded simultaneously per image sequence and analyzed separately off-line. Different colors were assigned to the individual terminals and to their calculated fluorescence changes in (d). (d) Downward and upward motion elicit changes in mean  $\text{Ca}^{2+}$  in individual terminals that are modulated at 1 Hz, the temporal frequency of the drifting grating ( $\lambda = 30$  deg, velocity = 30 deg/s,  $f = 1$  Hz, motion period 5 sec). Individual terminals signal the passing of the consecutive OFF-edges through their receptive field. From one terminal to the next, the signal modulation is phase shifted by  $\pi/3$  corresponding to the relationship of the spatial wavelength  $\lambda$  and the sampling base of the *Drosophila* eye ( $\Delta\phi = \sim 5$  deg). (e) Front-to-back (f-to-b) and back-to-front (b-to-f) motion elicit synchronous fluorescence changes in individual terminals at the temporal frequency of the drifting horizontal grating (grating same as in d, motion period 5 sec). (f) Gratings drifting horizontally in opposite directions with  $f = 1$  Hz (same as in e) as well as flickering stimuli (1 Hz) elicit similar fluorescence modulations. Upper trace: Front-to-back motion is followed by back-to-front motion. Middle trace: reverse sequence. Lower trace: 1 Hz flicker. All stimulus conditions elicit similar mean  $\text{Ca}^{2+}$  responses. Scale bars: 20  $\mu\text{m}$  in b and 10  $\mu\text{m}$  c and f, respectively. In d / e / f the plotted mean fluorescence signal was calculated from 23 / 20 / 20 image sequences that were recorded at the same position and animal. Similar experiments were performed in  $n = 6 / 5 / 6$  animals and 150 / 130 / 250 image sequences.

**Figure 4.** Genetic interference with the circuitry suggests that signal processing in L2 neurons is largely but not completely independent of photoreceptor-to-lamina signaling in parallel processing pathways. (a) Achromatic brightness information perceived by the outer photoreceptors R1-6 is transmitted to three direct pathways to the medulla (L1-L3) and two indirect pathways ( $\text{amc} \rightarrow \text{L5}$ ,  $\text{L2} \rightarrow \text{L4}$ ; only  $\text{amc}$  shown). L1-3 and  $\text{amc}$  (see introduction) express the histamine-gated chloride channel encoded by the gene  $\text{ort}^{30}$  and sense the photoreceptor transmitter histamine. Left: TN-XXL is specifically expressed in L2 cells ( $21D\text{-Gal4}^7$ ;  $\text{UAS-TN-XXL}^{42}$ ) in an otherwise wild type fly. Right: Mutations in the  $\text{ort}$  gene render  $\text{amc}$ , L1-L3 insensitive to histamine<sup>7</sup>. Photoreceptor-to-L2 signaling is specifically rescued and changes in  $\text{Ca}^{2+}$  in L2 are recorded by expressing the  $\text{ort}$  cDNA and TN-XXL in exclusively L2 cells in the optic lobe ( $\text{UAS-TN-XXL}^{42} / \text{UAS-ort}^7$ ;  $21D\text{-Gal4}^7$ ,  $\text{ort}^1 / \text{ort}^{\text{US2515}}$ ). (b) The onset of the first light pulse (1) induces a decrease in  $\text{Ca}^{2+}$  (asterisk). A characteristic strong increase in  $\text{Ca}^{2+}$  is observed at the offset of the first light pulse (black trace), this  $\text{Ca}^{2+}$  signal is rapidly reduced to baseline by the onset of a second pulse of light (inter stimulus interval  $\Delta t = 0.86$  s (orange) and 0.26 s (green);  $n = 3$  animals, 103 image sequences). (c) Decay of the OFF- $\text{Ca}^{2+}$  response in the reconstituted L2 pathway:  $\tau = 6.36$  for the simple OFF- $\text{Ca}^{2+}$  and 0.34 seconds for the OFF- $\text{Ca}^{2+}$  when truncated by a consecutive light-ON stimulus (single exponential fit to the data in panel c,  $R=0.97$  and 0.94, respectively). Compared to wild type  $\text{Ca}^{2+}$ -signals, the main characteristics of the  $\text{Ca}^{2+}$  response is retained in the reconstituted L2 pathway. However, interactions among parallel pathways are very likely as the time course of the recorded signal is significantly prolonged.

## METHODS SUMMARY

**Flies and 2-Photon Laser Scanning Microscopy.** The Gal4/UAS system, 21D-Gal4<sup>7</sup>, UAS-ort<sup>7</sup> and UAS-TN-XXL<sup>42</sup> were used to target all expression to L2 lamina monopolar cells. Within the imaged area in the optic lobes 21D-Gal4 driven expression was fairly specific for L2. Female flies were exclusively used in all experiments. Flies were dissected as described recently<sup>19</sup> with two differences: (a) no protease was used, and (b) 3 mM Ca<sup>2+</sup> instead of 1.5 mM Ca<sup>2+</sup> were contained in the ringer solution. L2 terminals in the medulla were imaged using a previously described custom-built Two-Photon microscope (design kindly provided by Winfried Denk) which allows for wide-field or Two-Photon imaging through the same objective (63x / 0.90 n.a., water immersion, IR Achromplan; Zeiss, Jena, Germany). Two-Photon fluorescence was excited by a mode-locked Ti:Sapphire laser (< 100 fs, 80 MHz, 700-1000 nm; pumped by a 10 W Millennia laser; both Tsunami; Spectraphysics, Darmstadt, Germany). Laser intensity was held constant at typically 5 and maximally 10 mW at the specimen. CFP of TN-XXL was selectively excited at 825 nm and CFP and YFP emission were recorded simultaneously (64 x 64 pixels; 128 ms / image) with two separate photomultipliers. Visual stimuli were programmed in Matlab (Vers. 7.3.0.267, The Mathworks, USA) and presented to the eye of the fly using a custom built LED arena<sup>19</sup> operating at four intensity levels.

**Interlaced visual stimulation.** A TTL signal generated at the beginning of each line-scan of the horizontal scanning mirror was used to trigger the individual panels of the LED arena. Stimuli were exclusively presented during 330  $\mu$ s of the 400  $\mu$ s fly-back period of the horizontal scanning mirror after the mirror having reached its final position (1.6 ms scanning / line). Image sequences of 10 cd / m<sup>2</sup> mean brightness (corresponding to 60 cd / m<sup>2</sup> during light-ON) were generated. Temporal switching between fluorescence recording and stimulus presentation was performed at a frequency of 500 Hz which is well above the flicker-fusion frequency of the *Drosophila* eye<sup>45</sup>.

**Imaging and data analysis.** In all calcium imaging experiments 4 - 6 neighbouring terminals were recorded per image sequence (64 x 64 pixels, 128ms, see above). Individual image sequences of about 20 sec were taken every 2 minutes, the sequences were separated by complete darkness. Thus, the eye was always fully adapted to the dark before onset of each recording trial. For the calculation of the fluorescence change the background fluorescence was subtracted in each recorded channel and a ratio movie was generated ( $R = (\text{YFP-background}) / (\text{CFP-background})$ ). The expression pattern and anatomy of TN-XXL expressing neurons was analyzed by recording image stacks (512 x 512 pixels per image) with  $\Delta z = 1 \mu\text{m}$ . Four images were taken and averaged at each z position. Data was analyzed using MBF-ImageJ (NIH) and Origin7.5 (Additive, Friedrichsdorf, Germany). Figures were prepared using Adobe Photoshop 8.0 (Adobe Systems, San Jose California, US).

**Supplementary Figure 1.** Block diagram of the original Hassenstein-Reichardt-Model<sup>12</sup> (HRM) of visual motion detection and two variants that involve half-wave rectification of the light stimulus. **(a)** Basic HRM as originally derived from an input-output analysis of optomotor behaviour<sup>12</sup>. The basic computational steps are: (1) detection of local changes in luminance by two input lines, both signaling brightness increments as well as decrements, (2) temporal delay of one of the two input signals (asymmetrical temporal filtering), (3) multiplication of the temporally delayed and the instantaneous signal of two neighbouring locations, (4) subtraction of the signals of the two half-detectors tuned to opposite preferred direction. **(b)** HRM variant as suggested by Franceschini and colleagues<sup>22,23</sup> with separate channels for the processing of positive and negative input signals. Half-wave rectification of the input signals and their wiring results in distinct ON-detectors and OFF-detectors. There are no interactions between positive and negative input signals. **(c)** HRM variant inspired by the “Four-Quadrant-Multiplier”<sup>12</sup> employed for the sign-correct multiplication of bipolar input signals in analog signal processing. Half-wave rectification and sorting of the input signals underlies four separate detectors for the detection of moving stimuli with all possible polarities (ON-ON, OFF-OFF, ON-OFF, OFF-ON). In contrast to the previous model, terms with mixed sign are not eliminated. The summed output of this model is mathematically identical to the model in (a).

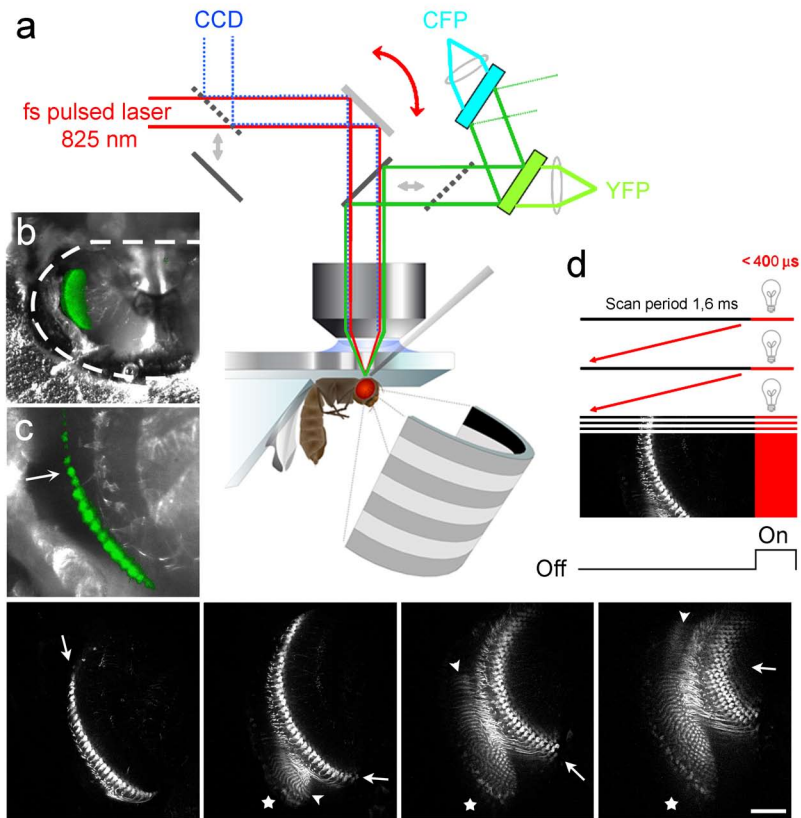
## Reference List

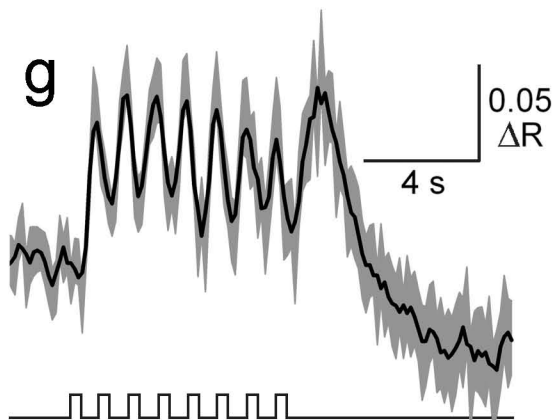
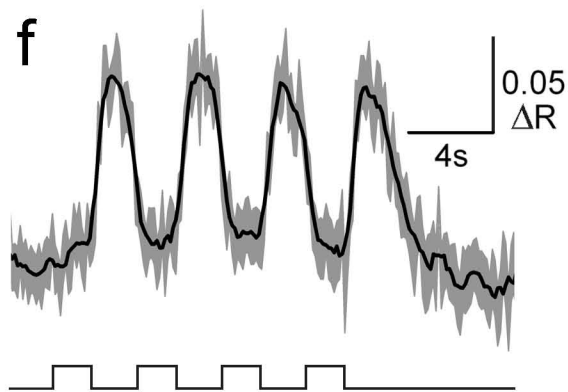
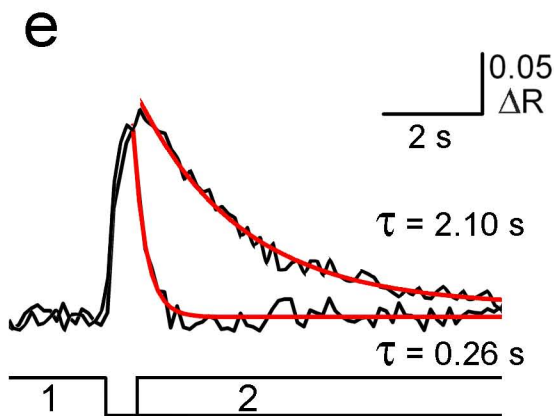
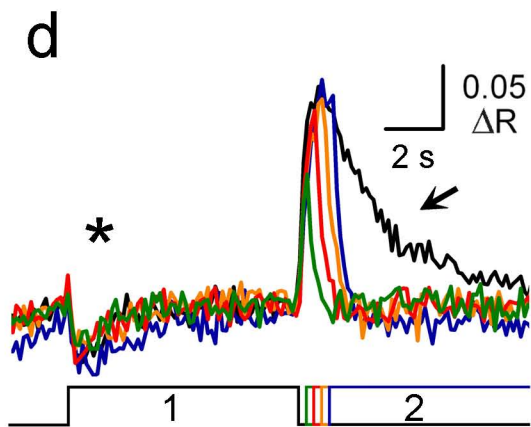
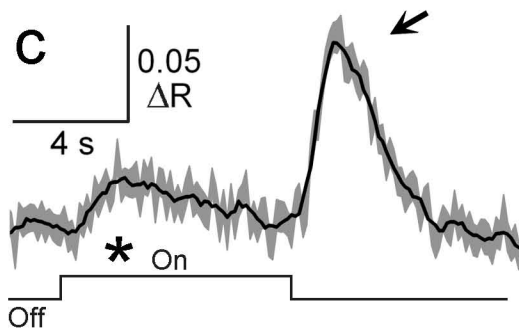
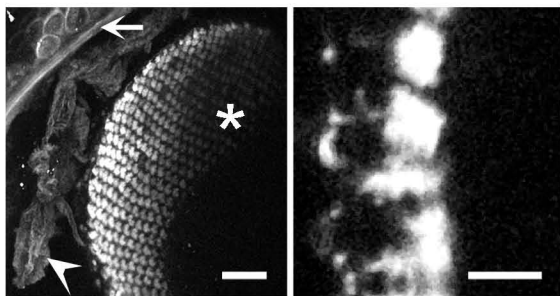
1. Tammero,L.F. & Dickinson,M.H. The influence of visual landscape on the free flight behavior of the fruit fly *Drosophila melanogaster*. *J. Exp. Biol.* **205**, 327-343 (2002).
2. Heisenberg,M. & Wolf,R. On the structure of yaw torque in visual flight orientation of *Drosophila melanogaster*. *J. Comp. Physiol. A* **130**, 113-130 (1979).
3. Tammero,L.F. & Dickinson,M.H. Collision-avoidance and landing responses are mediated by separate pathways in the fruit fly, *Drosophila melanogaster*. *J. Exp. Biol.* **205**, 2785-2798 (2002).
4. Mronz,M. & Lehmann,F.O. The free-flight response of *Drosophila* to motion of the visual environment. *J. Exp. Biol.* **211**, 2026-2045 (2008).
5. Borst,A. & Haag,J. Neural networks in the cockpit of the fly. *J. Comp. Physiol. A* **188**, 419-437 (2002).
6. Clifford,C.W. & Ibbotson,M.R. Fundamental mechanisms of visual motion detection: models, cells and functions. *Prog. Neurobiol.* **68**, 409-37 (2002).
7. Rister,J. *et al.* Dissection of the peripheral motion channel in the visual system of *Drosophila melanogaster*. *Neuron* **56**, 155-170 (2007).
8. Coombe,P.E. & Heisenberg,M. The structural brain mutant vacuolar medulla of *Drosophila melanogaster* with specific behavioral defects and cell degeneration in the adult. *J. Neurogenet.* **3**, 135-158 (1986).
9. Zhu,Y., Nern,A., Zipursky,S.L. & Frye,M.A. Peripheral visual circuits functionally segregate motion and phototaxis behaviors in the fly. *Curr. Biol.* **19**, 613-619 (2009).
10. Katsov,A.Y. & Clandinin,T.R. Motion processing streams in *Drosophila* are behaviorally specialized. *Neuron* **59**, 322-335 (2008).
11. Hassenstein,B. & Reichardt,W. Systemtheoretische Analyse einer Verhaltensweise (der Wechsel-Folgen-Reaktion des Rüsselkäfers *Chlorophanus viridis*). *Verh. Dtsch. Zool. Ges.* **7**, 95-102 (1952).
12. Hassenstein,B. & Reichardt,W. Systemtheoretische Analyse der Zeit-, Reihenfolgen- und Vorzeichenbewertung bei der Bewegungspertzeption des Rüsselkäfers *Chlorophanus*. *Z. Naturforsch.* **11b**, 513-524 (1956).
13. Götz,K.G. Optomotorische Untersuchungen des visuellen Systems einiger Augenmutanten der Fruchtfliege *Drosophila*. *Kybernetik* **2**, 77-92 (1964).
14. van Doorn,A.J. & Koenderink,J.J. Temporal properties of the visual detectability of moving spatial white noise. *Brain Res.* **45**, 179-188 (1982).

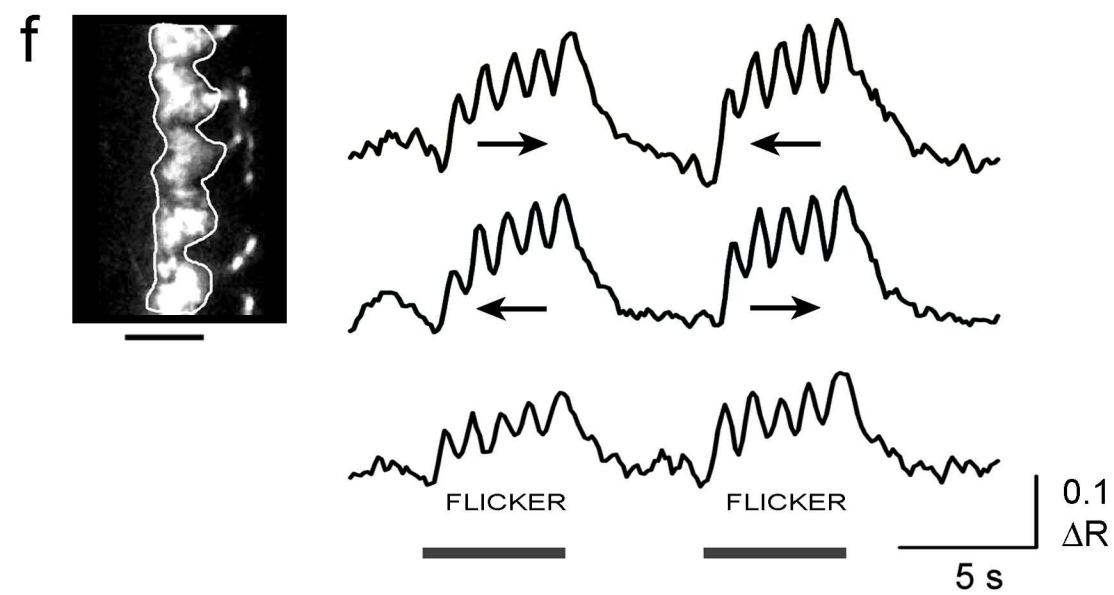
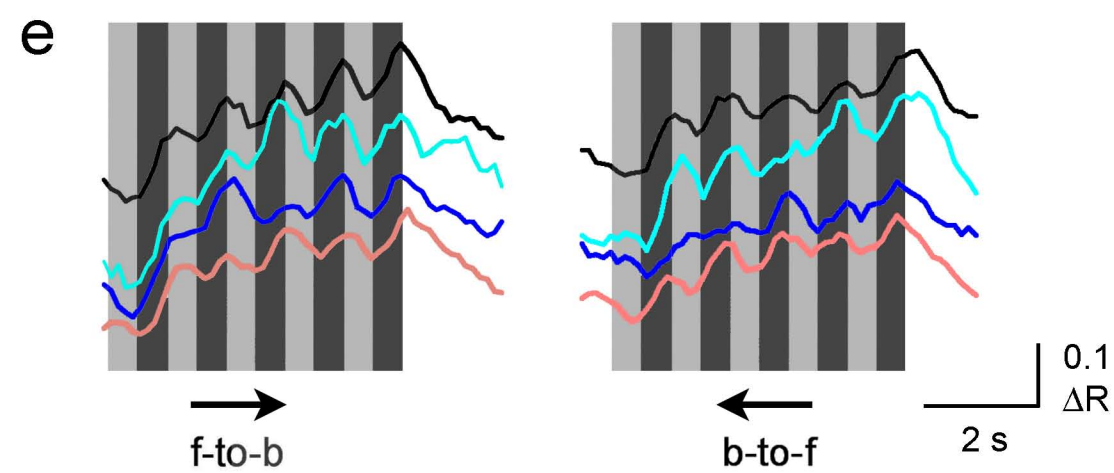
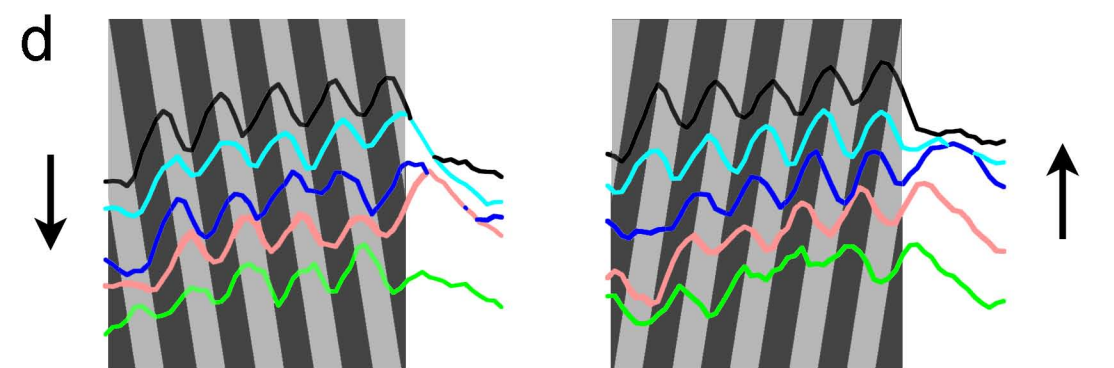
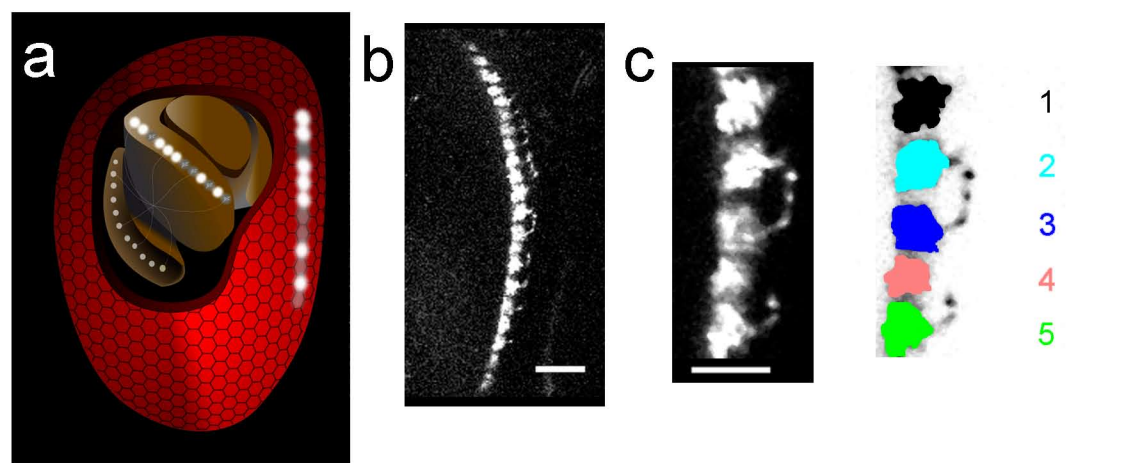
15. Barlow,H.B. & Levick,W.R. The mechanism of directionally selective units in rabbit's retina. *J. Physiol.* **178**, 477-504 (1965).
16. van Santen,J.P.H. & Sperling,G. Temporal covariance model of human motion perception. *J. Opt. Soc. Am. A* **1**, 451-473 (1984).
17. Adelson,E.H. & Bergen,J.R. Spatiotemporal energy models for the perception of motion. *J. Opt. Soc. Am. A* **2**, 284-299 (1985).
18. Borst,A., Haag,J. & Reiff,D.F. Fly Motion Vision. *Annu. Rev. Neurosci.* **33**, 49-70 (2010).
19. Joesch,M., Plett,J., Borst,A. & Reiff,D.F. Response properties of motion-sensitive visual interneurons in the lobula plate of *Drosophila melanogaster*. *Curr. Biol.* **18**, 1-7 (2008).
20. Schnell,B. *et al.* Processing of horizontal optic flow in three visual interneurons of the *Drosophila* brain. *J. Neurophysiol.* **103**, 1646-1657 (2010).
21. Egelhaaf,M. & Borst,A. Are there separate ON and OFF channels in fly motion vision? *Vis. Neurosci.* **8**, 151-164 (1992).
22. Franceschini,N., Riehle,A. & Le Nestour,A. Facets of vision. Stavenga,D.G. & Hardie,R.C. (eds.), pp. 360-390, Springer-Verlag, Berlin,Heidelberg (1989).
23. Riehle,A. & Franceschini,N. Motion detection in flies: parametric control over ON-OFF pathways. *Exp. Brain Res.* **54**, 390-394 (1984).
24. Ullman,S. The interpretation of visual motion. Cambridge, MA: MIT Press, (1979).
25. Anstis,S.M. & Rogers,B.J. Illusory reversals of visual depth and movement during changes in contrast. *Vis.Res.* **15**, 957-961 (1975).
26. Takemura,S.Y., Lu,Z. & Meinertzhagen,I.A. Synaptic circuits of the *Drosophila* optic lobe: the input terminals to the medulla. *J. Comp. Neurol.* **509**, 493-513 (2008).
27. Strausfeld,N.J. Atlas of an insect brain. Springer, Berlin, Heidelberg (1976).
28. Fischbach,K.F. & Dittrich,A.P.M. The optic lobe of *Drosophila melanogaster*. I. A Golgi analysis of wild-type structure. *Cell Tissue Res.* **258**, 441-475 (1989).
29. Meinertzhagen,I.A. & O'Neil,S.D. Synaptic organization of columnar elements in the lamina of the wild type in *Drosophila melanogaster*. *J. Comp. Neurol.* **305**, 232-263 (1991).
30. Gengs,C. *et al.* The target of *Drosophila* photoreceptor synaptic transmission is a histamine-gated chloride channel encoded by ort (hclA). *J. Biol. Chem.* **277**, 42113-42120 (2002).

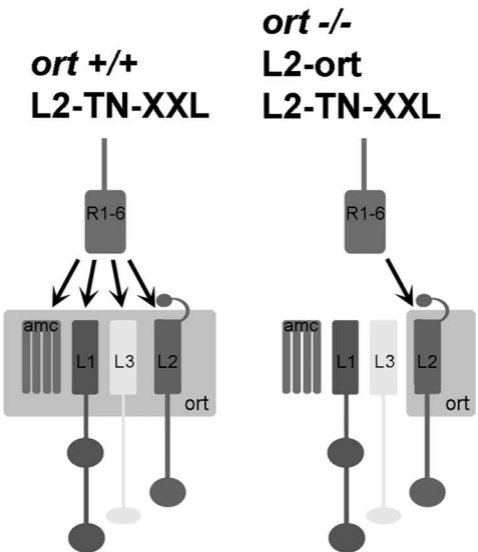
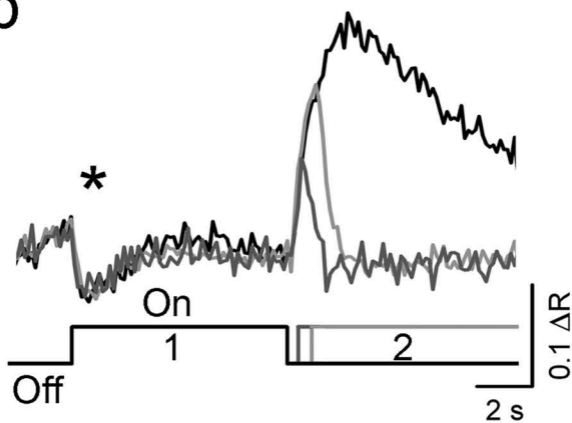
31. Hardie,R.C. A histamine-activated chloride channel involved in neurotransmission at a photoreceptor synapse. *Nature* **339**, 704-706 (1989).
32. Skingsley,D.R., Laughlin,S.B. & Hardie,R.C. Properties of histamine-activated chloride channels in the large monopolar cells of the dipteran compound eye: a comparative study. *J. Comp. Physiol. A* **176**, 611-623 (1995).
33. Laughlin,S.B. & Osorio,D. Mechanism for neural signal enhancement in the blowfly compound eye. *J. Exp. Biol.* **144**, 113-146 (1989).
34. Jarvilehto,M. & Zettler,F. Electrophysiological-histological studies on some functional properties of visual cells and second order neurons of an insect retina. *Z. Zellforsch. Mikrosk. Anat.* **136**, 291-306 (1973).
35. Zettler,F. & Järvillehto,M. Lateral inhibition in an insect eye. *Z. vergl. Physiologie* **76**, 233-244 (1972).
36. Zettler,F. & Järvillehto,M. Active and passive axonal propagation of non-spike signals in the retina of *Calliphora*. *J. Comp. Physiol.* **85**, 89-104 (1973).
37. Zettler,F. & Straka,H. Synaptic chloride channels generating hyperpolarizing on-responses in monopolar neurons of the blowfly visual system. *J. Exp. Biol.* **131**, 435-438 (1987).
38. Zheng,L. *et al.* Feedback network controls photoreceptor output at the layer of first visual synapses in *Drosophila*. *J. Gen. Physiol.* **127**, 495-510 (2006).
39. Douglass,J.K. & Strausfeld,N.J. Visual motion detection circuits in flies: peripheral motion computation by identified small-field retinotopic neurons. *J. Neurosci.* **15**, 5596-5611 (1995).
40. Douglass,J.K. & Strausfeld,N.J. Visual motion-detection circuits in flies: parallel direction- and non-direction-sensitive pathways between the medulla and lobula plate. *J. Neurosci.* **16**, 4551-4562 (1996).
41. Buschbeck,E.K. & Strausfeld,N.J. Visual motion-detection circuits in flies: small-field retinotopic elements responding to motion are evolutionarily conserved across taxa. *J. Neurosci.* **16**, 4563-4578 (1996).
42. Mank,M. *et al.* A genetically encoded calcium indicator for chronic in vivo two-photon imaging. *Nat. Methods* (2008).
43. Denk,W., Strickler,J.H. & Webb,W.W. Two-photon laser scanning fluorescence microscopy. *Science* **248**, 73-76 (1990).
44. Euler,T., Detwiler,P.B. & Denk,W. Directionally selective calcium signals in dendrites of starburst amacrine cells. *Nature* **418**, 845-852 (2002).
45. Wu,C.F. & Wong,F. Frequency characteristics in the visual system of *Drosophila*: genetic dissection of electroretinogram components. *J. Gen. Physiol.* **69**, 705-724 (1977).

46. Coombe,P.E. The large monopolar cells L1 and L2 are responsible for ERG transients in *Drosophila*. *J. Comp. Physiol. A* **159**, 655-665 (1986).
47. Wassle,H. Parallel processing in the mammalian retina. *Nat. Rev. Neurosci.* **5**, 747-757 (2004).
48. Molnar,A., Hsueh,H.A., Roska,B. & Werblin,F.S. Crossover inhibition in the retina: circuitry that compensates for nonlinear rectifying synaptic transmission. *J. Comput. Neurosci.* **27**, 569-590 (2009).
49. Renteria,R.C. *et al.* Intrinsic ON responses of the retinal OFF pathway are suppressed by the ON pathway. *J. Neurosci.* **26**, 11857-11869 (2006).
50. Suzuki,H., Thiele,T.R., Faumont,S., Ezcurra,M., Lockery,S.R. & Schafer,W.R. Functional asymmetry in *Caenorhabditis elegans* taste neurons and its computational role in chemotaxis. *Nature* **454**, 114-117 (2008).







**a****b****c**